*34th EPS Conference on Plasma Phys. Warsaw, 2 - 6 July 2007 ECA Vol.**31F**, P-1.041 (2007)*

Evolution of Be migration after Be evaporation in the JET tokamak

K. Krieger[a], M. Stamp[b], S. Brezinsek[c], H.G. Esser[c], S. Jachmich[b], A. Kreter[c], S. Menmuir[d], Ph. Mertens[c], V. Philipps[c], P. Sundelin[d] and JET EFDA contributors[*]

[a]*Max-Planck-Institut f. Plasmaphysik, Assoc. EURATOM-IPP, Garching, Germany*

[b]*Euratom/UKAEA Fusion Assoc., Culham Science Centre, Oxon OX14 3DB, UK*

[c]*Inst. f. Energieforsch., FZJ, EURATOM Assoc., Trilateral Euregio Cluster, Jülich, Germany*

[d]*Association EURATOM - VR, Fusion Plasma Physics, EES, KTH, Stockholm, Sweden*

INTRODUCTION

Beryllium will be used as main chamber armour material for ITER. Migration and re-deposition of eroded Beryllium is considered a potential hazard because Be might contribute to formation of tritium inventories by co-deposition and because of possible deterioration of tungsten armour by alloy formation with Be. In previous studies at JET, campaign integrated Be and C sources at the main chamber wall were compared to post campaign deposition measurements at retrieved divertor tiles [1]. It turned out that both materials are predominantly deposited in the inner divertor. This observation can be interpreted as a consequence of erosion dominating at outer divertor and main chamber wall and migration of eroded material to the inner divertor following the experimentally observed plasma boundary flow pattern. To study the time scales of the corresponding erosion and migration processes in more detail and to obtain data suitable for benchmarking of impurity transport modelling, dedicated experiments with focus on a particular discharge scenario are required. L-mode discharges are particularly useful for this purpose because they allow avoiding the additional complication of ELMs.

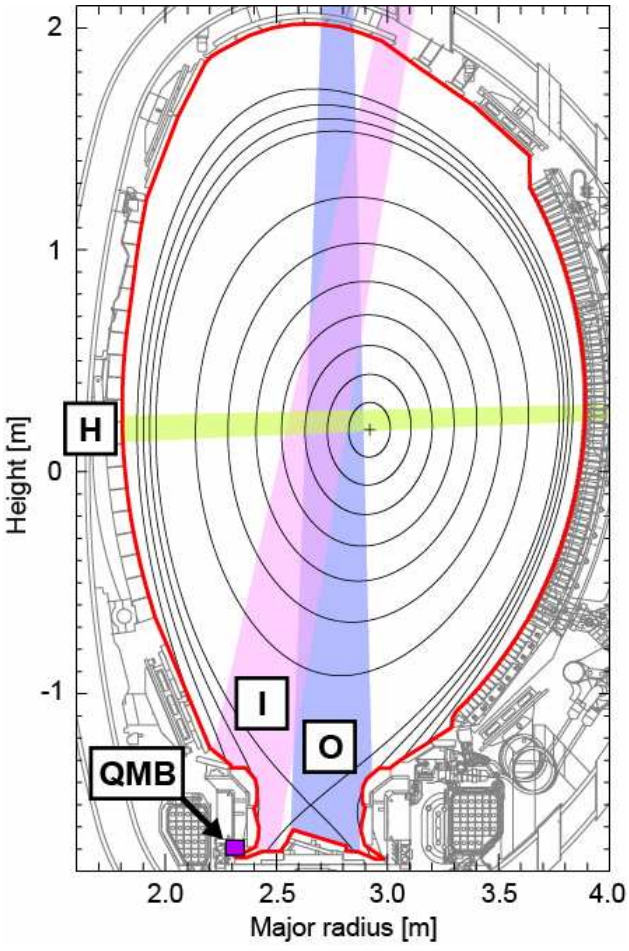

Figure 1: Poloidal cross-section of JET with observation positions of visible range spectrometers at main chamber wall and divertor target plates. Flux surfaces in the plot correspond to the flat-top phase of the L-mode discharges.

DIAGNOSTIC SETUP

Local Be and C sources were measured spectroscopically in the visible spectral range. The evolution of Be II , C II and D_β line intensities from discharge to discharge allows to derive estimates for the relative change of beryllium and carbon surface concentration. Figure 1 shows respective lines of sight of the JET KS3A spectrometer viewing at the inner (I) and outer (O) divertor and horizontally at the mid-plane main chamber wall (H). Viewing chord H at the plasma mid-plane was additionally supplied to a high resolution Mechelle spectrometer for separate determination of inboard and outboard wall sources by Zeeman analysis. Charge exchange spectrometry was used to measure the evolution of the carbon plasma concentration. Furthermore, the material deposition rate at the inner divertor was detected by a quartz microbalance (QMB).

DISCHARGE SCENARIO

A series of 15 identical 2.5MA, 2.4T L-mode discharges with 1.5MW neutral beam heating was run after 4 hour Be evaporation with elevated evaporator temperature (1000°C vs. 850°C default) to achieve maximum Be wall coverage. The wall status before Be evaporation was documented by a reference discharge with identical configuration at the end of the preceding session. To avoid excessive local erosion in the main chamber, the plasma shape (Figure 1) was tailored to ensure sufficient wall clearance and the discharge schedule was programmed without limiter start-up phase and as early as possible X-point formation. A low triangularity configuration with strike points at the horizontal target plates was used to adjust the position of the divertor impurity source to the available spectroscopic viewing chords. Each discharge had ≈10 s flat top time with ≈7 seconds neutral beam heating and stationary plasma wall clearance and strike point positions.

BERYLLIUM AND CARBON SOURCES

With constant plasma flux and plasma temperature local Be II and C II line intensities normalised to the intensity of the D_β Balmer line provide a suitable measure for the respective surface fraction. Figure 2 shows the evolution of the normalised Be II (527.1nm) line intensity during the discharge series for the mid-plane main chamber wall (H) and for the outer (O) and inner (I) divertor. The data points represent the signal average in the time window from 48.5-49.5s during the neutral beam heated plasma phase. Both at main chamber wall and outer divertor region one observes a factor 6-8 increase relative to the pre-Be evaporation level decreasing by ≈30% (H) and ≈50% (O) in the first 3 discharges and subsequently followed by a slower continuous decrease over the remaining 12 discharges of the experiment. In contrast, the Be signal from the inner divertor increased only by a factor 3 over the level before Be

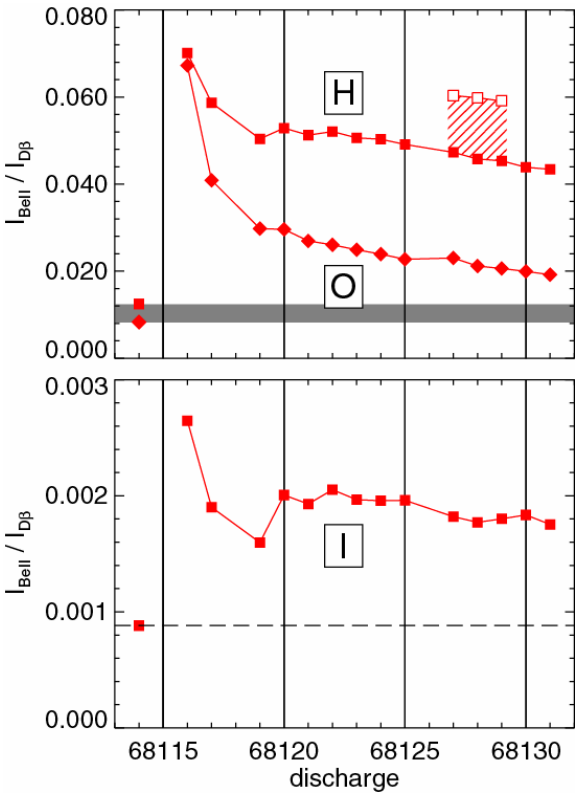

Figure 2: Evolution of Be II intensity normalised to D_β for main chamber (H), outer (O) and inner divertor (I). The hatched area denotes the effect of a 6 cm plasma shift towards the central wall.

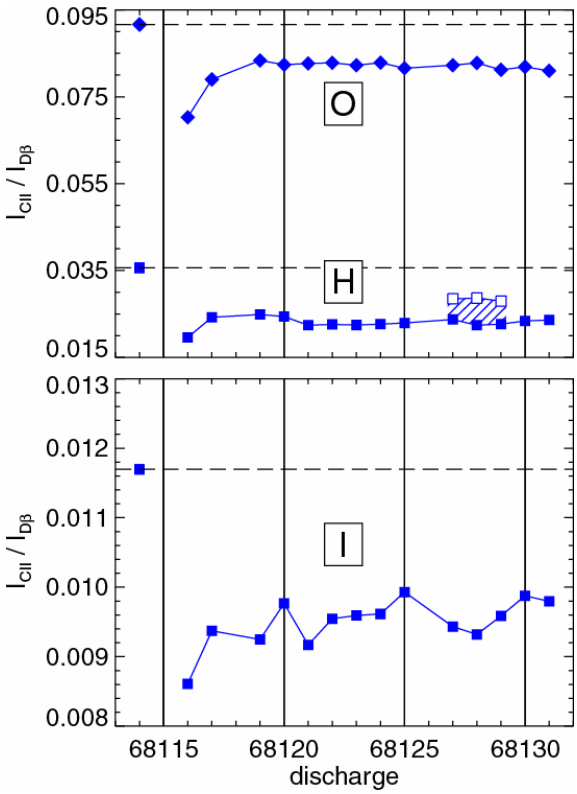

Figure 3: Evolution of C II intensity normalised to D_β for main chamber (H), outer (O) and inner divertor (I). The hatched area denotes the effect of a 6 cm plasma shift towards the central wall.

evaporation and also showed a significantly lower decrease rate than the main chamber and outer divertor Be II signals.

On the carbon sources the effect of the Be evaporation is opposite to the beryllium behaviour. Figure 3 shows, as in Figure 2 for beryllium, the C II (589.1nm) line intensity normalised to the D_β intensity. At the main chamber wall, the CII signal drops by ≈45% after Be evaporation and reaches steady state after the first two discharges. A similar behaviour is observed in the divertor, however with a smaller drop of ≈45%. Correspondingly, the deposition rate at the inner divertor measured by quartz microbalance remained, after a slight initial increase in the first 4 discharges, constant during the experiment. The results show that the preceding Be evaporation procedure did not result in complete Be wall coverage. A possible explanation is the 150°C lower temperature of the Be evaporator in JET vessel octant 1 where the visible range spectrometers are located. The resulting toroidal asymmetry will be analysed in detail by numerical tracing of the evaporated Be to the plasma facing wall. First results of Zeeman line splitting analysis at the mid-plane position (H) show approximately equal source strength at inboard and outboard wall for both carbon and the beryllium.

CARBON PLASMA CONCENTRATION

Spectroscopic erosion flux measurements can only provide data for a few selected vessel locations. A more global quantity is the plasma concentration of a given impurity, which is directly correlated to the product of erosion flux and screening factor averaged over the entire wall area. Figure 4 shows the evolution of the carbon concentration, f_C, at two radial positions. As in Figure 2 and Figure 3, the data points represent averages in the time window 48.5-49.5 s. The drop of the carbon concentration after Be evaporation and the following increase rate are similar to the corresponding evolution of the local C II source rates. In 3 discharges, the plasma was also shifted by 6 cm towards the central wall. This leads to increased erosion of Be and C at the central column (Figure 2 and Figure 3), however, at the same time the carbon concentration decreases significantly. From these observations one infers that carbon sources at the outboard wall and limiters contribute much more to the carbon level in the plasma than C sources at the central column.

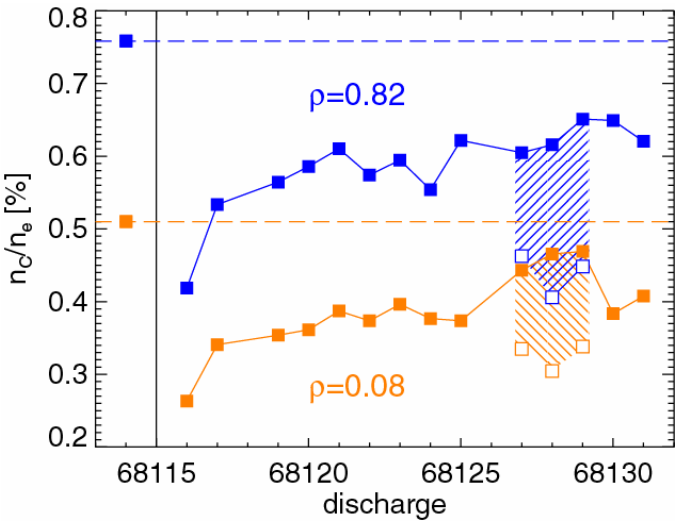

Figure 4: Evolution of carbon plasma concentration $f_C=n_C/n_e$ in plasma centre (normalised radius ρ=0.08) and outer plasma region (ρ=0.82). The hatched areas denote the effect of a 6 cm plasma shift towards the central wall.

CONCLUSIONS

Post-campaign analysis of Be coverage on retrieved divertor tiles showed Be deposition mainly at the inner divertor. This observation, combined with similar results for carbon, indicates that redeposition prevails over gross erosion in the inner divertor while the outer target plate is a region of Be net erosion. Consequently, one would expect a smaller impact of Be evaporation on the Be source in the inner divertor compared to erosion dominated wall regions. This is qualitatively confirmed by the results of the current experiment, where the Be sources at both the main chamber wall and the outer divertor show much stronger variations than in the inner divertor. Impurity transport simulations will be required for quantitative interpretation of the new results to improve the current model of the Be migration path.

[1] G.F. Matthews, J. Nucl. Mat., 337–339 (2005) 1–9.

*See Appendix of M.L.Watkins et al., Proc. 21st Int. Conf. Chengdu, 2006, IAEA (2006).